ACS APPLIED MATERIALS & INTERFACES

Research Article

www.acsami.org

Synthesis of Copper Graphene Materials Functionalized by Amino Acids and Their Catalytic Applications

Qiang Huang, Limei Zhou,* Xiaohui Jiang, Yafen Zhou, Hongwei Fan, and Wencheng Lang

Chemical Synthesis and Pollution Control Key Laboratory of Sichuan Province, China West Normal University, Nanchong, Sichuan 637002, People's Republic of China

Supporting Information

ABSTRACT: Graphene oxide and its derivative have attracted extensive interests in many fields, including catalytic chemistry, organic synthesis, and electrochemistry, recently. We explored whether the use of graphene after chemical modification with amino acids to immobilize copper nanoparticles could achieve a more excellent catalytic activity for N-arylation reactions. A facile and novel method to prepare copper supported on amino-acid-grafted graphene hybrid materials (A−G−Cu) was first reported. The as-prepared hybrid materials were characterized by a variety of techniques, including Fourier transform infrared spectroscopy, X-ray photoelectron spectroscopy, X-ray diffraction, scanning electron microscopy, atomic force microscopy, transmission electron microscopy, and inductively coupled plasma−atomic emission spectrometry. The results showed that the morphology, distribution, and loading of copper nanoparticles could be well-adjusted by controlling the type of amino acids grafted on graphene. Moreover, most A−G−Cu hybrid materials could catalyze N-arylation of imidazole with iodobenzene with yields more than 90%, while the copper supported on graphene (G−Cu) displayed a yield of just 65.8%. The high activity of A−G−Cu can be ascribed to the good synergistic effects of copper nanoparticles (Cu NPs) and amino-acid-grafted graphene.

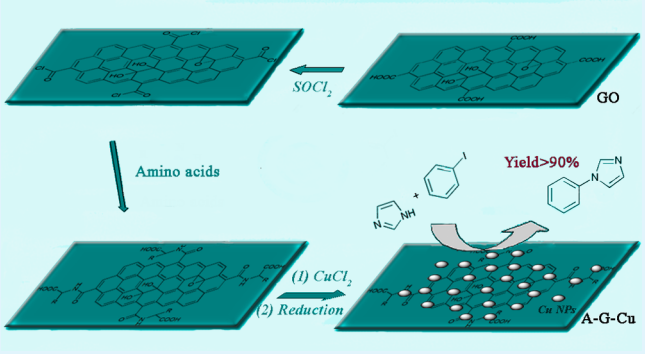

KEYWORDS: *functionalized graphene, copper, catalyst, amino acids, N-arylation*

1. INTRODUCTION

Graphene oxide (GO), a novel and promising two-dimensional (2D) carbon nanomaterial, has attracted extensive attention in catalysis fields, such as photochemistry, electrochemistry, and organic catalysis, for the past few years.[1−5] Graphene-based materials hold unique features, such as large surface, high water dispersibility, intrinsic low mass, easy surface modifications, and ample oxygen-carrying functionalities,[6−8] which might be promising candidates as catalysts or supports. Among the chemical methods, harsh oxidation of the graphite is the most versatile and easily scalable method that can be used to prepare GO.[9] Obviously, GO exhibits an excellent hydrophilic nature, owing to the enrichment of oxygen-carrying functional groups on its basal planes and edges.[10] These functional groups and defects allow GO to be readily functionalized with various surfactants, polymer, alkaloid, organometallic compounds, and metal nanoparticles,[11−14] which are highly favorable for catalysis applications using these materials as supports or catalysts. In addition, to immobilize organometallic compounds or nanoparticles on functionalized graphene is also very important for recovery and recyclability of catalysts.

Up to the above point, some investigations about GO after chemical or physical modification as catalysis materials for organic synthesis and catalysis were reported recently.[15−18] For example, after chemical modification of GO with oxo-vanadium Schiff base, the composite was noted as highly efficient for the oxidation of various alcohols, diols, and α-hydroxyketones to carbonyl compounds using *tert*-butyl hydroperoxide (TBHP) as an oxidant.[15] Pristine L-proline was non-covalently loaded on the GO sheet in a simple route by mixing them in aqueous solution, giving the excellent L-proline/GO catalyst for the direct asymmetric aldol reaction.[16] In 2013, Wang et al. first reported that a N-heterocyclic carbine−palladium complex (NHC−Pd^{2+}) was immobilized on the surface of GO via a chemical-bonding method as a novel catalyst for the Suzuki−Miyaura reaction.[17] Furthermore, a cross-dehydrogenative coupling reaction between tertiary amines and nitroalkanes had been realized in water simply using graphene-supported RuO_2 as the catalyst.[18] To the best of our knowledge, few reports exist about a functionalized graphene material by amino acids via a covalent chemical bond. Although Silvia et al. investigated the preparation of graphene and silver graphene hybrids by natural bioreductants, such as pyridoxine, pyridoxamine, and vitamin B_2, as well as the amino acids arginine, histidine, and tryptophan,[19] these biomolecules were inevitably decomposed into some small molecules through redox reaction.

Received: April 28, 2014
Accepted: July 31, 2014
Published: July 31, 2014

Scheme 1. Synthesis of A−G−Cu Hybrids and Application in N-Arylation of Imidazole with Iodobenzene

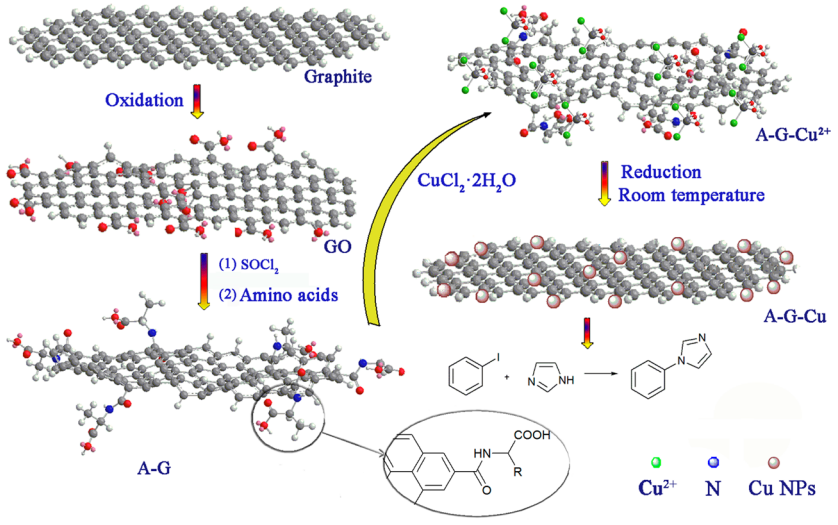

Consequently, we attempted to establish a protocol to prepare different amino-acid-grafted graphene (A−G) as a support because of a good coordination interaction between amino acids and metal ions,[20] which can be rather conducive to improve the catalytic performance of metal particles on the supports.

In the past few years, copper-assisted Ullmann-type coupling reactions were extensively explored by using amino acids as ligands to promote these coupling reactions in Ma's research groups.[21−23] They considered that the structure of α-amino acids could accelerate Cu-assisted Ullmann reactions, leading to the coupling reactions of aryl halides and α-amino acids under mild conditions.[21] However, these homogeneous systems have limited their practical applications because of product contamination as a direct result of an inability to effectively separate the catalyst from the reaction product. Herein, considering the easy surface modifications of GO and excellent coordination ability of amino acids, the implementation of novel approaches toward the preparation of copper supported on the α-amino-acid-functionalized graphene materials (A−G−Cu) was proposed in our work. We first reported a practical Cu-catalyzed N-arylation of imidazole using different A−G−Cu hybrids as the heterogeneous catalysts and also systematically compared and optimized the performance of A−G−Cu materials. Meanwhile, the morphology and distribution of copper nanoparticles could be well-adjusted by controlling the type of amino-acid-grafted graphene. In addition, the route for grafting various amino acids on graphene nanolayers is fairly convenient and cheap, and then the amino-acid-grafted graphene samples can be produced on a large scale through simple chemical treatment.

2. EXPERIMENTAL SECTION

2.1. Materials and Instrumentations. All of the information about the materials and instrumentations used in this study was displayed in the Supporting Information.

2.2. Synthesis of GO. GO was synthesized from natural graphite powder by a modified Hummers method.[9] The detailed procedures were showed in the Supporting Information.

2.3. Preparation of Amino-Acid-Functionalized Graphene Hybrids. The whole route of preparation was shown in Scheme 1. Typically, GO (30 mg) was treated with $SOCl_2$ (20 mL) in the presence of 0.5 mL of dry *N*,*N*-dimethylformamide (DMF) in a 50 mL round-bottomed flask and heated to 70 °C for 24 h, using an absorption device of neutralization tail gas. After completion of the reaction, the solvent was evaporated at 100 °C and the solid was washed by anhydrous tetrahydrofuran (THF). The obtained product was reacted with amino acids (2.0 mmol) in anhydrous DMF (20 mL) at 90 °C for 12 h. The amino-acid-grafted graphene sheets were obtained by filtration and washed by 5 wt % Na_2CO_3 or NaOH, deionized water, and ethanol to remove the unreacted amino acids, respectively, and finally dried under vacuum at 50 °C. The different amino-acid-grafted graphene materials were uniformly labeled as A−G.

2.4. Synthesis of Different Graphene-Based Cu Catalysts. The different A−G materials were added to the 0.05 mg mL^{-1} $CuCl_2$ solution with stirring (Cu ∼ 10 wt % in theory) and then sonicated to obtain the homogeneous suspension. Subsequently, the 1.0 mg mL^{-1} $NaBH_4$ solution was added dropwise into the above solution for 2 h by the constant flow pump under ambient conditions. The mixture was then aged for 24 h under magnetic stirring and recovered by filtration, followed by washing with distilled water and dry ethanol, respectively. The precipitate was finally dried at 50 °C for 12 h under vacuum.

2.5. N-Arylation Reaction Catalyzed by A−G−Cu Catalysts. A total of 1.0 mmol of iodobenzene, 1.2 mmol of imidazole, 2.0 mmol of base, and 5.0 mg of catalyst were placed in the reaction vessel. Then, 2 mL of dimethyl sulfoxide (DMSO) was added with the protection of nitrogen. The reaction mixture was heated fast to 110 °C in an oil bath and kept at this temperature for 24 h. After cooling to room temperature, the reaction mixture was analyzed by gas chromatography (GC).

3. RESULTS AND DISCUSSION

3.1. Preparation and Characterization of the A−G−Cu Catalysts. In the process of designing the new A−G−Cu catalysts, we used amino acids to adjust functionalization of graphene and the growth of Cu nanoparticles (Cu NPs) on the surface of the functionalized graphene. The structures of amino acids and abbreviation of catalysts were listed (as seen in Tables S3 and S4 of the Supporting Information).

First, the as-prepared typical materials, such as Lys−G−Cu and His−G−Cu, were characterized by Fourier transform infrared spectroscopy (FTIR) analysis. As seen from Figure 1, aromatic C═C and C═O stretching vibrations in the GO materials was obvious at near 1631.3 and 1745.8 cm^{-1} and the strong peaks around 3441.8 and 1400 cm^{-1} partially ascribe to absorbed water. The peaks at 1045 cm^{-1} can be attributed to the alkoxy C−O stretching vibration.[24] After grafting amino acids on the GO material, the peaks at 1212.1, 1577.6, and

dx.doi.org/10.1021/am502586c | ACS Appl. Mater. Interfaces 2014, 6, 13502−13509

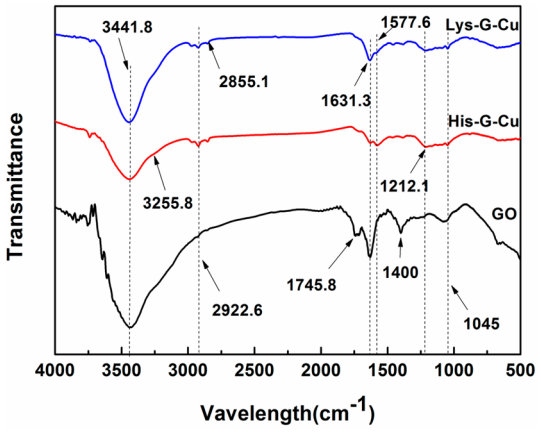

Figure 1. FTIR spectra of GO, His−G−Cu, and Lys−G−Cu samples.

1631.3 cm^{-1} are attributed to characteristic amide bonds.[14,25] Furthermore, the presence of a multiplet at 2922.6 and 2855.1 cm^{-1} was associated with the stretching vibrations of CH_2 that exist on the amino acids. These results showed that a successful functionalization by amino acids had in fact occurred.

In addition, the FTIR analysis of other A−G−Cu catalysts was shown in Figure S1 of the Supporting Information. Similar results could be obtained. Hence, the result suggested that the amino acids had been covalently grafted to the graphene sheets successfully through a simple chemical reaction.

Additional qualitative evidence for the installation of surface-bound amide groups was obtained through X-ray photoelectron spectroscopy (XPS) analysis of His−G−Cu and Lys−G−Cu catalysts. The C 1s spectra were deconvoluted into four main peaks at 284.5, 285.6, 286.6, and 288.4 eV in panels a and b of Figure 2, which were attributed to C−C/C═C, C−N, C−O,

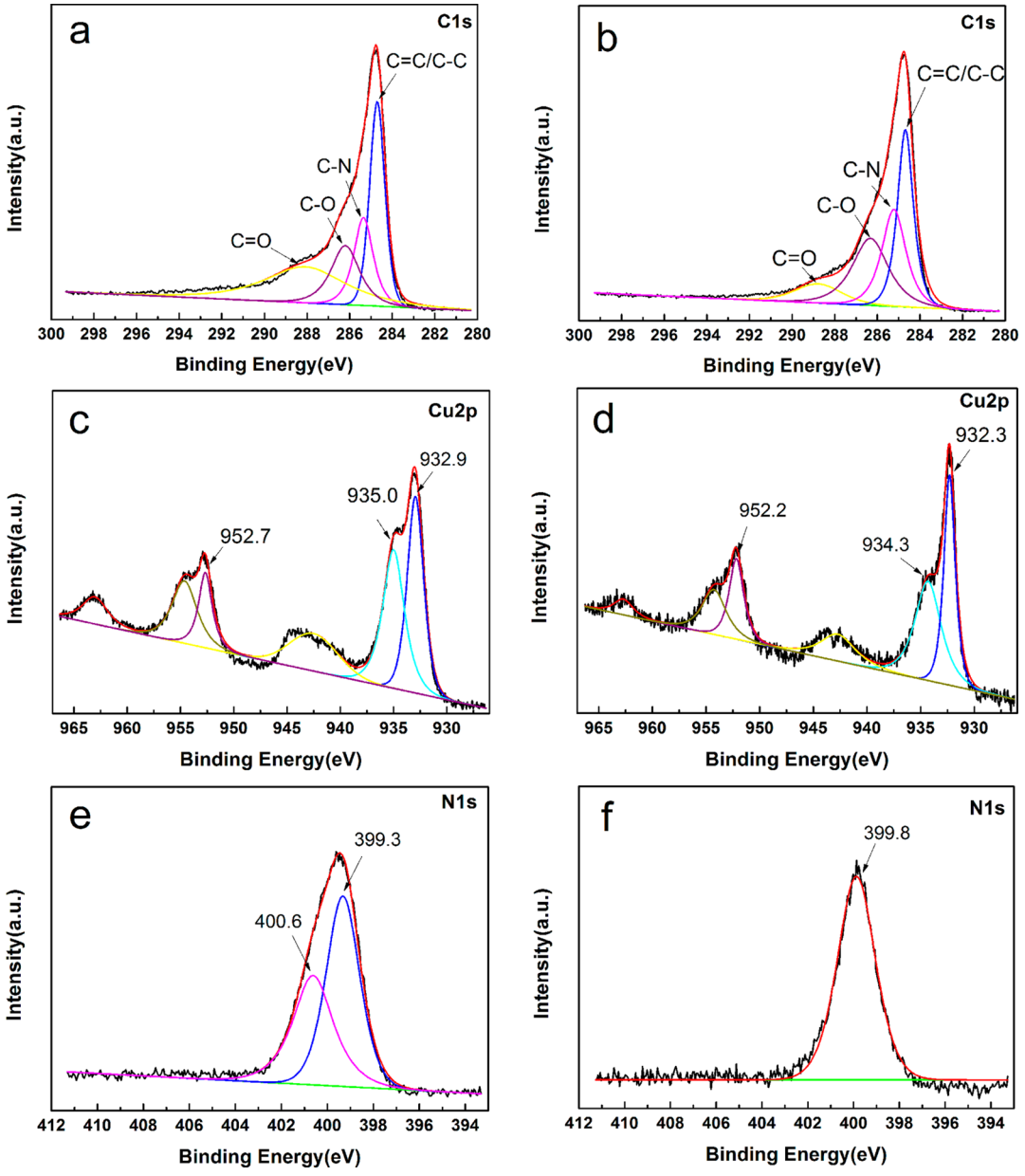

Figure 2. XPS analysis of catalysts: C 1s spectra of (a) His−G−Cu and (b) Lys−G−Cu, Cu 2p spectra of (c) His−G−Cu and (d) Lys−G−Cu, and N 1s spectra of (e) His−G−Cu and (f) Lys−G−Cu.

and C═O, respectively.[26] Moreover, the N 1s spectrum is used to determine the nitrogen configuration. The N 1s spectra could be divided into two peaks for His−G−Cu material in Figure 2e, one peak at 399.3 eV ascribed to sp^2 nitrogen in the imidazole ring and another 400.6 eV peak attributed to the amine N of the His−G−Cu composite.[27,28] In contrast, one type of nitrogen was observed at 399.8 eV for Lys−G−Cu material in Figure 2f, which was assigned to amine N species.[29]

Furthermore, the valence states of copper on different hybrid surfaces were confirmed by the XPS analysis in panels c and d of Figure 2. It was clear that copper was in the Cu^{2+}, Cu^{+}, and Cu^{0} components. To the best of our knowledge, Cu^{0} and Cu^{+} are hard to discriminate because they have ∼0.3 eV separation in binding energy, whereas Cu^{0} and Cu^{2+} have more than 2 eV separations.[30] Therefore, the dominant Cu $2p_{3/2}$ peak at 932.9 eV could be assigned to Cu^{0} or Cu^{+}, whereas the small peak at 935.0 eV could be assigned to Cu^{2+} for the His−G−Cu catalyst.[31] In contrast, the binding energy of Cu $2p_{3/2}$ in the Lys−G−Cu composite decreased from 932.9 and 935.0 eV to 932.3 and 934.3 eV, correspondingly. However, the calculated intensity ratio of $Cu^{+/0}$ and Cu^{2+} ($Cu^{+/0}/Cu^{2+}$) in the His−G−Cu and Lys−G−Cu catalysts were 1.15 and 1.38, respectively. Results showed that the higher reduction degree of copper components occurred when L-lysine was grafted on the graphene sheets. The main reason was attributed to the stronger interaction between L-histidine and divalent copper, so that the further reduction of copper bound on the L-histidine-grafted graphene (His−G) was more difficult.

X-ray diffraction (XRD) of the GO, His−G−Cu, and Lys−G−Cu materials further confirmed the crystalline structures of the Cu NPs and graphene, as shown in Figure 3. Obviously, a

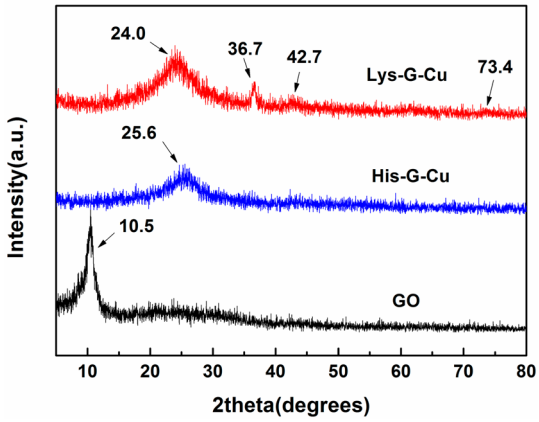

Figure 3. XRD plots of the GO, His−G−Cu, and Lys−G−Cu materials.

diffraction peak of GO (001) that appeared at $2\theta = 10.5°$ was observed with d spacing of 0.84 nm.[32] The XRD peak at 10.5° completely disappeared after reduction in the His−G−Cu and Lys−G−Cu materials, but there was a significant amount of C═O groups left from XPS results in panels a and b of Figure 2. This result indicated the reduction of GO and the restoration of the sp^2 carbon sites in the His−G−Cu and Lys−G−Cu materials, and some C═O groups in these materials could be assigned to carboxyl and amide groups that could not be reduced by $NaBH_4$. Additional carboxyl groups would be introduced when amino acids were grafted on GO; therefore, the amount of C═O groups would increase. Additionally, a new peak at about 25° could belong to the stacking of graphene layers after GO was functionalized by different amino acids. For the His−G−Cu material, no obvious diffraction peaks of copper were detected in Figure 3. However, inductively coupled plasma (ICP) analysis showed that the amount of copper in the sample was about 9.7 wt %. In contrast, the diffraction peaks of Cu_2O (200), Cu_2O (111), and Cu (220) in the Lys−G−Cu catalyst were clear at 42.7°, 36.7°, and 73.4°, respectively.[33]

The crystal structures of the other A−G−Cu materials were also investigated by XRD (see Table S6 and Figure S2 of the Supporting Information). Interestingly, the diffraction peaks of copper were not present in the functionalized graphene by grafting L-histidine, L-glutamic acid, and L-tryptophan on the GO sheets, while the Cu species on other supports could be detected in Table S6 of the Supporting Information. Obviously, crystalline structures and valence state of copper should be diverse from the results of XRD analysis of different A−G−Cu catalysts. For instance, with regard to the Tyr−G−Cu catalyst, the peaks at 32.1° (220) and 29.4° (110) were consistent with CuO and Cu_2O species, respectively, and the coalescence of two crystallites was recognized at 48.2° (204) in Figure S2a of the Supporting Information.[33] Moreover, for Phe−G−Cu, Gly−G−Cu, and Thr−G−Cu materials, the only diffraction peak of pure Cu crystals was detected at 43.3° (111) in Figure S2b of the Supporting Information. The peaks of Pro−G−Cu at 36.7° (111) and 43.3° (111) could belong to Cu_2O and Cu NPs, respectively.

Generally, the sharp and intensive peaks indicated a highly organized crystal structure of Cu NPs,[25] whereas the diffraction peak of amorphous nanoparticles was weak, caused by the line broadening of the XRD peak.[34] XRD analysis of the A−G−Cu catalysts implied that the structure of different amino acids could result in the difference in crystal structure of Cu NPs. For example, for His−G−Cu or Trp−G−Cu materials, when amino acids with imidazole or indole groups were grafted on the graphene, strong coordination interaction between Cu^{2+} and attachment sites of amino acids decreased the degree of reduction, which resulted in forming amorphous nanoparticles[35] (Figure 6 and Figure S3 of the Supporting Information). In contrast, for Phe−G−Cu or Lys−G−Cu materials, an organized crystal structure of Cu NPs could be obtained because of the weak interaction.

In this research, the morphology of the typical products was further investigated by scanning electron microscopy (SEM), atomic force microscopy (AFM), and transmission electron microscopy (TEM). Figure 4 showed the typical SEM images of the GO, functionalized graphene, and copper catalyst nanostructures. The 2D composite nanosheets with wrinkled and folded features could be clearly observed in the GO and Lys−G materials. However, the stacking of His−G−Cu and Lys−G−Cu hybrids was much larger than that of GO, which could be attributed to the interaction of amino acid groups at the periphery or in the basal plane of GO.

AFM is a powerful tool to measure the thickness of the samples. Figure 5 showed the AFM images of the GO, Lys−G, and Lys−G−Cu materials. The thickness of the GO nanosheet was 1.14 nm. After grafting L-lysine on the graphene, the thickness of the hybrid was much larger than GO sheets in panels b and c of Figure 5. At the same time, the thickness of the Lys−G−Cu hybrid increased from 3.37 to 3.75 nm by immobilizing Cu NPs on the Lys−G support. The increase of the thickness may be due to cross-linking by amino acids bound on the graphene. However, the green arrow directed that the

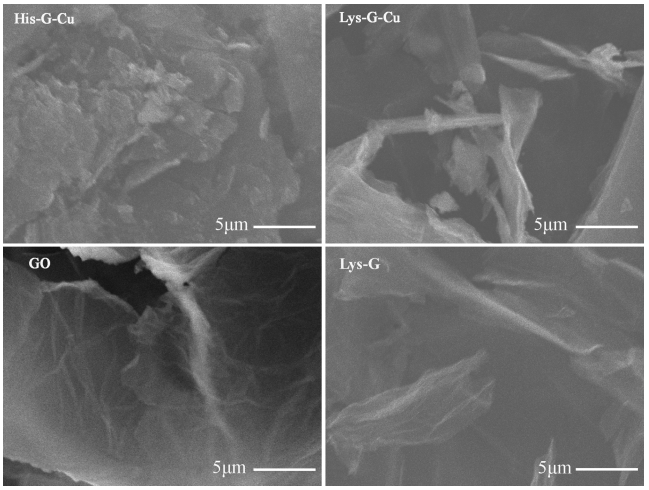

Figure 4. SEM images of the His−G−Cu and Lys−G−Cu catalysts, GO, and Lys−G at 5 μm size magnification.

thickness of Lys−G−Cu materials was 8.4 nm in Figure 5c. The increase of thickness may be caused by deposition of Cu NPs on the amino-acid-grafted graphene.

Furthermore, according to the results of XRD characterization, the morphology of Cu NPs on the different supports should be diverse. Hence, the as-prepared typical materials, such as Lys−G−Cu and His−G−Cu, were characterized by TEM (as seen in Figure 6). The Cu NPs on the surface of the His−G−Cu catalyst were amorphous-like worms (panels a and c of Figure 6). However, a homogeneous dispersion of Cu NPs was observed for the Lys−G−Cu hybrid. TEM showed the presence of ∼10 nm size Cu NPs in large numbers on the graphene surface, and the Cu NPs were mainly spherical (panels b and d of Figure 6).

The different morphologies between Lys−G−Cu and His−G−Cu may be related to the different amino acids. For the Lys−G−Cu materials, copper ions (Cu^{2+}) can first complex with the N sites of the L-lysine-grafted graphene hybrid,[36]

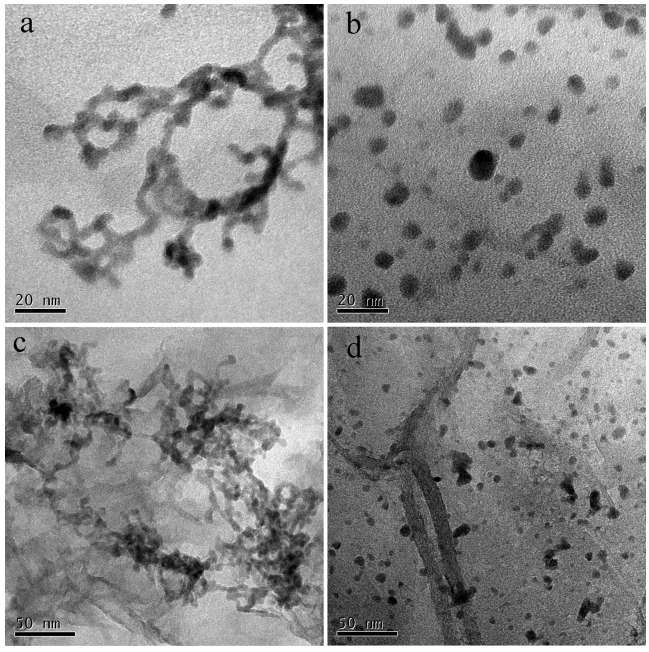

Figure 6. TEM images of the as-prepared (a and c) His−G−Cu and (b and d) Lys−G−Cu at different magnifications.

followed by reduction of Cu^{2+} ions to Cu^0 by controlled addition of $NaBH_4$, and the individual Cu NPs can be obtained. In contrast, for His−G−Cu material, the wormlike Cu NPs can be observed, it can be explained that L-histidine-grafted graphene has N sites and a π-conjugated system, and the multiple attachment sites can result in extensive aggregation of Cu NPs. The explanation could also be supported by TEM images of other A−G−Cu hybrids in Figure S3 of the Supporting Information. We found that the aggregation of Cu NPs was obvious on these materials with rich N sites or a π-conjugated system, such as Arg−G−Cu, Tyr−G−Cu, and Trp−G−Cu hybrid materials.

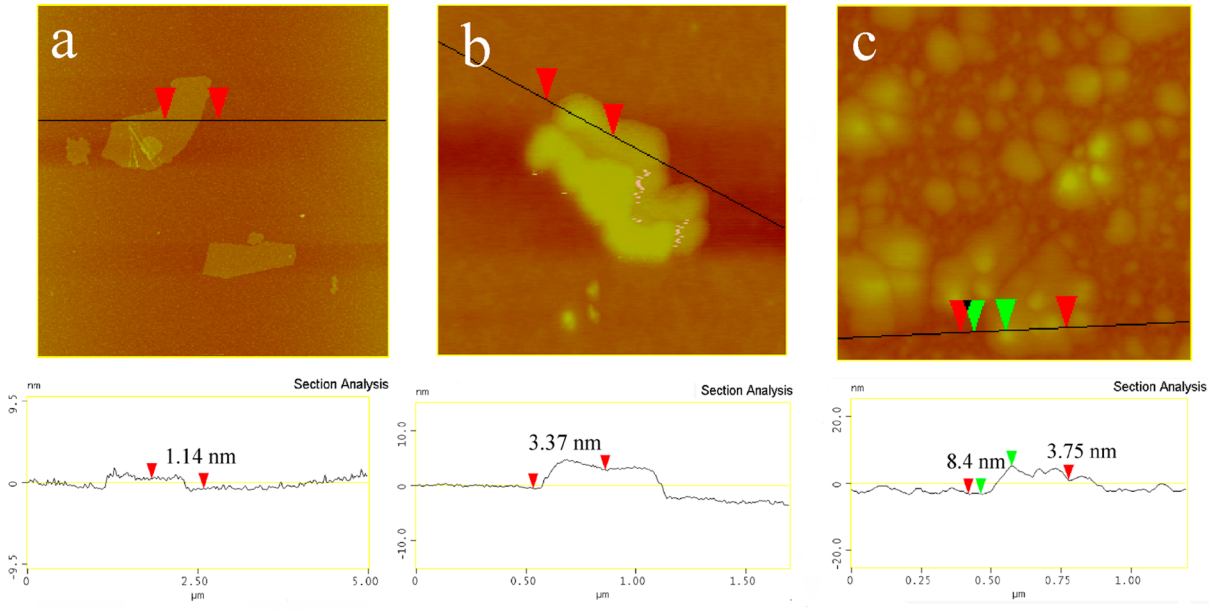

Figure 5. AFM height images of (a) GO in ethanol, (b) Lys−G in ethanol, and (c) Lys−G−Cu samples in ethanol.

To elucidate the quantitative correlation between amino acids and copper species, copper loading in the graphene-based composites was determined from the acid extract of the sample using inductively coupled plasma−atomic emission spectroscopy (ICP−AES) in Table 1. Interestingly, high loading of copper was obtained in these materials, such as Tyr−G−Cu, Trp−G−Cu, Lys−G−Cu, Arg−G−Cu, and His−G−Cu. In comparison to other amino acids, these amino acids include either a rich amine group or aromatic ring active sites, which could be considered to be the main driving force for the affinity for Cu^{2+} ions. However, for Glu−G−Cu material, the lowest amount of copper was detected, which may be attributed to acidity of carboxyl groups that was bad for immobilizing copper particles. Because L-glutamic acid is an acidic amino acid, the H^+ ions from carboxyl groups can hinder the adsorption of Cu^{2+} ions, resulting in low copper loading. For the Pro−G−Cu catalyst, copper loading was just 7.8 wt %. It may be reasonable that the specific structure of L-proline grafted on graphene had a bearing on immobilization of metals. Cu^{2+} ions in the solution were hard to find close to the attachment sites of the support because of the immobilization of the pyrrolidine ring of L-proline.

Table 1. Comparison of the Catalytic Performance for N-Arylation Reaction of Imidazole with Iodobenzene Using Different Catalysts[a]

entry	catalyst	amino acid	loading of Cu (wt %)	yield (%)[b]
1	Gly−G−Cu	glycine	8.2	94.1
2	Phe−G−Cu	L-phenylalanine	8.3	95.8
3	Thr−G−Cu	L-threonine	8.6	94.4
4	Tyr−G−Cu	L-tyrosine	9.7	93.2
5	Pro−G−Cu	L-proline	7.8	54.6
6	Trp−G−Cu	L-tryptophan	9.6	83.3
7	Lys−G−Cu	L-lysine	9.8	93.8
8	Arg−G−Cu	L-arginine	10.0	90.6
9	His−G−Cu	L-histidine	9.7	94.3
10	Glu−G−Cu	L-glutamic acid	6.4	79.7
11	G−Cu		9.5	65.8

[a]Reaction conditions: aryl halide, 1 mmol; imidazole, 1.2 mmol; NaOH, 2 mmol; A−G−Cu, 5 mg; DMSO, 2 mL; *t*, 24 h; and *T*, 110 °C. [b]GC yield.

Finally, the dispersion experiment of GO and A−G−Cu hybrid materials was added in Figure S4 of the Supporting Information. The results showed that GO can be well-dispersed in DMSO. Most A−G−Cu materials can also be dispersed in this solvent.

3.2. Catalytic Performance of A−G−Cu Catalysts. Generally, it is of great significance to research the use range of a novel material in the practical application, such as electrochemistry and organic catalysis areas. Hence, to evaluate the catalytic activity of the A−G−Cu hybrids in organic synthesis, N-arylation of imidazole with iodobenzene was investigated in Scheme 2.

First, to identify the best system for this reaction, the Tyr−G−Cu material as a catalyst in conjunction with different bases was screened in Table S5 of the Supporting Information. Notably, in the controlled experiments of the reaction conditions, the optimal system for the coupling reactions was obtained using KOH as the base at 110 °C (entry 3). Furthermore, the effect of the reaction temperature was also investigated. When Tyr−G−Cu was used as the catalyst, the iodobenzene conversion ranged between 62.8 and 93.2% using NaOH as the base with the increasing temperature from 90 to 110 °C (entries 2, 9, and 10). Therefore, considering the low price of NaOH, the optimum conditions were as follows: 5 mg of A−G−Cu, 2 mmol of NaOH as the base, and DMSO as the solvent at 110 °C under an atmosphere of nitrogen.

Scheme 2. N-Arylation of Imidazole with Iodobenzene

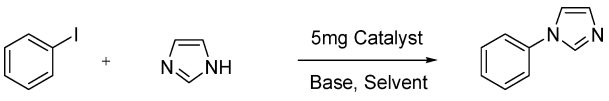

Next, it is instructive to compare the catalytic performance of different materials chemically functionalized by various amino acids. As shown in Table 1, we were delighted to find that most A−G−Cu hybrids as catalysts showed very high activity (>90%) for the N-arylation reaction compared to the unmodified copper graphene catalyst (G−Cu). This result suggested that the amino acids that covalently grafted graphene can further improve the performance of copper nanoparticles on supports. According to early literature, Ma et al. in 2003 reported that the structures of α- and β-amino acids could induce acceleration of Ullmann-type aryl amination.[21,23] Herein, we speculated that a synergistic effect of amino acids should play an important role for controlling catalytic performance of Cu NPs in the N-arylation reaction. Similar synergistic effects were reported in previous literature.[37,38] However, for the Pro−G−Cu catalyst, a 54.6% yield of product was obtained. Because amide bond formation between the pyrrolidine group of L-proline and the carboxy group of GOs resulted in the low flexibility of the pyrrolidine ring, this specific structure generated a big steric hindrance between the amide N sites and active Cu NPs. Hence, the synergistic effect of amino acid did not work. In contrast, a slightly good yield (79.7%) of product was obtained using Glu−G−Cu as the catalyst (entries 5 and 10). Low copper loading may be the main influence factor for the activity of the Glu−G−Cu catalyst.

Meanwhile, the amorphous Cu NPs could give comparable catalytic performance as the crystalline structure in this reaction. The catalytic performance of Cu NPs may be related to the structure of amino acids. The morphology of Cu NPs can be adjusted by grafting different amino acids on the GO, while good performance of catalysts can also be achieved by a synergistic effect of amino acids. Herein, the synergistic effect of amino acids may play an important role for controlling the catalytic performance of Cu NPs.

In this work, A−G−Cu hybrid materials as catalysts could further enhance the catalysis performance. As shown in Table 2, when the active copper species were immobilized on the surface

Table 2. Comparison of Activity of Different Heterogeneous Copper Catalysts in the N-Arylation Reaction

entry	catalyst	condition	yield (%)	reference
1	CuO/AB	5 mol % Cu, KO^{t}Bu, toluene, and 180 °C	100	39
2	[Cu]/Meso-N-C-1	15 mol % Cu, KOH, DMSO, and 125 °C	88	29
3	CuO	1.26 mol % Cu, KOH, DMSO, and 110 °C	91	40
4	Cu_2O	10 mol % Cu, KOH, DMSO, and 110 °C	90	41
5	Tyr−G−Cu	0.76 mol % Cu, NaOH, DMSO, and 110 °C	93	this study

of functionalized graphene, an enhanced performance could be achieved for N-arylation compared to the unmodified graphene catalyst. Meanwhile, the low amount of catalyst is remarkable to studies reported to date. Furthermore, graphene after chemical modification as a support is superior to other support materials, such as Meso-N-C-1 (entry 2 in Table 2).

4. CONCLUSION

In summary, we have developed a facile and novel method to prepare copper amino-acid-grafted graphene hybrid materials. Interestingly, the morphology, distribution, and loading of Cu NPs could be well-controlled through grafting the graphene with different amino acids, and the enhanced catalytic performance was achieved for N-arylation compared to the unmodified graphene catalyst. Because the structure of α-amino acids can accelerate Cu-assisted Ullmann reactions, high performance should be tentatively explained as a good synergistic effect of copper nanoparticles and amino-acid-grafted graphene. However, the catalytic mechanism is not quite clear from this material as a catalyst, and a further investigation is still extremely urgent for these new catalyst materials. Furthermore, the as-obtained novel A−G−Cu catalysts can be not only applied to organic catalysis but also used possibly in other areas, such as photocatalysis, electrochemistry, and biochemistry. From these results, the amino-acid-grafted graphene hybrid materials can be very promising substitutes for heterogeneous catalysts.

■ ASSOCIATED CONTENT

Ⓢ Supporting Information

Synthesis of GO, infrared (IR) spectra of A−G−Cu hybrids, and XRD patterns of A−G−Cu hybrids. This material is available free of charge via the Internet at http://pubs.acs.org.

■ AUTHOR INFORMATION

Corresponding Author

*Telephone: +86-817-2568081. E-mail: cwnuzhoulimei@163.com.

Notes

The authors declare no competing financial interest.

■ ACKNOWLEDGMENTS

The authors are grateful for financial support from the Natural Science Foundation of China (21303139), the Educational Department of Sichuan Province (11ZA035), and the Open Project of Chemical Synthesis and Pollution Control Key Laboratory of Sichuan Province (CSPC2010-3).

■ REFERENCES

(1) Li, B.; Cao, H.; Shao, J.; Li, G.; Qu, M.; Yin, G. Co_3O_4@graphene composites as anode materials for high-performance lithium ion batteries. *Inorg. Chem.* **2011**, *50*, 1628−1632.

(2) Shang, N.; Feng, C.; Zhang, H.; Gao, S.; Tang, R.; Wang, C.; Wang, Z. Suzuki−Miyaura reaction catalyzed by graphene oxide supported palladium nanoparticles. *Catal. Commun.* **2013**, *40*, 111−115.

(3) Yan, J.; Wang, Z.; Wang, H.; Jiang, Q. Rapid and energy-efficient synthesis of a graphene−CuCo hybrid as a high performance catalyst. *J. Mater. Chem.* **2012**, *22*, 10990−10993.

(4) Chen, Q.; Zhang, L.; Chen, G. Facile preparation of graphene−copper nanoparticle composite by in situ chemical reduction for electrochemical sensing of carbohydrates. *Anal. Chem.* **2012**, *84*, 171−178.

(5) Zhang, Y.; Tian, J.; Li, H.; Wang, L.; Qin, X.; Asiri, A.; Al-Youbi, A.; Sun, X. Biomolecule-assisted, environmentally friendly, one-pot synthesis of CuS/reduced graphene oxide nanocomposites with enhanced photocatalytic performance. *Langmuir* **2012**, *28*, 12893−12900.

(6) Chen, W.; Yan, L.; Bangal, P. Chemical reduction of graphene oxide to graphene by sulfur-containing compounds. *J. Phys. Chem. C* **2010**, *114*, 19885−19890.

(7) Garg, B.; Ling, Y. Versatilities of graphene-based catalysts in organic transformations. *Green Mater.* **2013**, *1*, 47−61.

(8) Bekyarova, E.; Itkis, M.; Ramesh, P.; Berger, C.; Sprinkle, M.; Heer, W.; Haddon, R. Chemical modification of epitaxial graphene: Spontaneous grafting of aryl groups. *J. Am. Chem. Soc.* **2009**, *131*, 1336−1337.

(9) Hummers, W.; Offeman, R. Preparation of graphitic oxide. *J. Am. Chem. Soc.* **1958**, *80*, 1339.

(10) Si, Y.; Samulski, E. Synthesis of water soluble graphene. *Nano Lett.* **2008**, *8*, 1679−1682.

(11) He, H.; Gao, C. General approach to individually dispersed highly soluble and conductive graphene nanosheets functionalized by nitrene chemistry. *Chem. Mater.* **2010**, *22*, 5054−5064.

(12) Georgakilas, V.; Bourlinos, A.; Zboril, R.; Steriotis, T.; Dallas, P.; Stubos, A.; Trapalis, C. Organic functionalisation of graphenes. *Chem. Commun. (Cambridge, U. K.)* **2010**, *46*, 1766−1768.

(13) Kerscher, B.; Appel, A.; Thomann, R.; Mülhaupt, R. Treelike polymeric ionic liquids grafted onto graphene nanosheets. *Macromolecules* **2013**, *46*, 4395−4402.

(14) Deng, S.; Tjoa, V.; Fan, H.; Tan, H.; Sayle, D.; Olivo, M.; Mhaisalkar, S.; Wei, J.; Sow, C. Reduced graphene oxide conjugated Cu_2O nanowire mesocrystals for high-performance NO_2 gas sensor. *J. Am. Chem. Soc.* **2012**, *134*, 4905−4917.

(15) Mungse, H.; Verma, S.; Kumar, N.; Sain, B.; Khatri, O. Grafting of oxo-vanadium Schiff base on graphene nanosheets and its catalytic activity for the oxidation of alcohols. *J. Mater. Chem.* **2012**, *22*, 5427−5433.

(16) Tan, R.; Li, C.; Luo, J.; Kong, Y.; Zheng, W.; Yin, D. An effective heterogeneous L-proline catalyst for the direct asymmetric aldol reaction using graphene oxide as support. *J. Catal.* **2013**, *298*, 138−147.

(17) Shang, N.; Gao, S.; Feng, C.; Zhang, H.; Wang, C.; Wang, Z. Graphene oxide supported N-heterocyclic carbene−palladium as a novel catalyst for the Suzuki−Miyaura reaction. *RSC Adv.* **2013**, *3*, 21863−21868.

(18) Meng, Q.; Liu, Q.; Zhong, J.; Zhang, H.; Li, Z.; Chen, B.; Tung, C.; Wu, L. Graphene-supported RuO_2 nanoparticles for efficient aerobic cross-dehydrogenative coupling reaction in water. *Org. Lett.* **2012**, *14*, 5992−5995.

(19) Fernández-Merino, M.; Villar-Rodil, S.; Paredes, J.; Solís-Fernández, P.; Guardia, L.; García, R.; Martínez-Alonso, A.; Tascón, J. Identifying efficient natural bioreductants for the preparation of graphene and graphene−metal nanoparticle hybrids with enhanced catalytic activity from graphite oxide. *Carbon* **2013**, *63*, 30−44.

(20) Chen, W.; Zhang, Y.; Zhu, L.; Lan, J.; Xie, R.; You, J. A concept of supported amino acid ionic liquids and their application in metal scavenging and heterogeneous catalysis. *J. Am. Chem. Soc.* **2007**, *129*, 13879−13886.

(21) Ma, D.; Cai, Q. Copper/amino acid catalyzed cross-couplings of aryl and vinyl halides with nucleophiles. *Acc. Chem. Res.* **2008**, *41*, 1450−1460.

(22) Chen, Y.; Xie, X.; Ma, D. Facile access to polysubstituted indoles via a cascade Cu-catalyzed arylation−condensation process. *J. Org. Chem.* **2007**, *72*, 9329−9334.

(23) Ma, D.; Cai, Q.; Zhang, H. Mild method for Ullmann coupling reaction of amines and aryl halides. *Org. Lett.* **2003**, *5*, 2453−2455.

(24) Chen, D.; Li, L.; Guo, L. An environment-friendly preparation of reduced graphene oxide nanosheets via amino acid. *Nanotechnology* **2011**, *22*, 325601−325608.

(25) Ouyang, Y.; Cai, X.; Shi, Q.; Liu, L.; Wan, D.; Tan, S.; Ouyang, Y. Poly-L-lysine-modified reduced graphene oxide stabilizes the copper

nanoparticles with higher water-solubility and long-term additively antibacterial activity. *Colloids Surf., B* **2013**, *107*, 107−114.
(26) Wu, T.; Wang, X.; Qiu, H.; Gao, J.; Wang, W.; Liu, Y. Graphene oxide reduced and modified by soft nanoparticles and its catalysis of the Knoevenagel condensation. *J. Mater. Chem.* **2012**, *22*, 4772−4779.
(27) Movahed, S.; Esmatpoursalmani, R.; Bazgir, A. N-Heterocyclic carbene palladium complex supported on ionic liquid-modified graphene oxide as an efficient and recyclable catalyst for Suzuki reaction. *RSC Adv.* **2014**, *4*, 14586−14593.
(28) Li, Z.; Liu, J.; Huang, Z.; Yang, Y.; Xia, C.; Li, F. One-pot synthesis of Pd nanoparticle catalysts supported on N-doped carbon and application in the domino carbonylation. *ACS Catal.* **2013**, *3*, 839−845.
(29) Zhang, P.; Yuan, J.; Li, H.; Liu, X.; Xu, X.; Antonietti, M.; Wang, Y. Mesoporous nitrogen-doped carbon for copper-mediated Ullmann-type C−O/−N/−S cross-coupling reactions. *RSC Adv.* **2013**, *3*, 1890−1895.
(30) Mondal, P.; Sinha, A.; Salam, N.; Roy, A.; Jana, N.; Islam, S. Enhanced catalytic performance by copper nanoparticle-graphene based composite. *RSC Adv.* **2013**, *3*, 5615−5623.
(31) Qi, X.; Zhou, L.; Jiang, X.; Fan, H.; Fu, H.; Chen, H. Montmorillonite-supported copper(I) for catalyzing N-arylation of nitrogen heterocycles. *Chin. J. Catal.* **2012**, *33*, 1877−1882.
(32) Qu, K.; Wu, L.; Ren, J.; Qu, X. Natural DNA-modified graphene/Pd nanoparticles as highly active catalyst for formic acid electro-oxidation and for the Suzuki reaction. *ACS Appl. Mater. Interfaces* **2012**, *4*, 5001−5009.
(33) Fakhri, P.; Jaleh, B.; Nasrollahzadeh, M. Synthesis and characterization of copper nanoparticles supported on reduced graphene oxide as a highly active and recyclable catalyst for the synthesis of formamides and primary amines. *J. Mol. Catal. A: Chem.* **2014**, *383*−*384*, 17−22.
(34) Liu, X.; Zhang, J.; Guo, X.; Wu, S.; Wang, S. Amino acid-assisted one-pot assembly of Au, Pt nanoparticles onto one-dimensional ZnO microrods. *Nanoscale* **2010**, *2*, 1178−1184.
(35) Deng, D.; Jin, Y.; Cheng, Y.; Qi, T.; Xiao, F. Copper nanoparticles: Aqueous phase synthesis and conductive films fabrication at low sintering temperature. *ACS Appl. Mater. Interfaces* **2013**, *5*, 3839−3846.
(36) Kumara, M.; Tripp, B.; Muralidharan, S. Self-assembly of metal nanoparticles and nanotubes on bioengineered flagella scaffolds. *Chem. Mater.* **2007**, *19*, 2056−2064.
(37) Li, Z.; Wu, S.; Zheng, D.; Ding, H.; Wang, X.; Yang, X.; Huo, Q.; Guan, J.; Kan, Q. Enhanced aerobic epoxidation of styrene with copper(II), cobalt(II), iron(III), or oxovanadium(IV) salen complexes immobilized onto carbon-coated Fe_3O_4 nanoparticles hybridized with graphene sheets. *ChemPlusChem* **2014**, *79*, 716−724.
(38) Ke, H.; Chen, X.; Zou, G. N-Heterocyclic carbene/phosphite synergistically assisted Pd/C-catalyzed Suzuki coupling of aryl chlorides. *Appl. Organomet. Chem.* **2014**, *28*, 54−60.
(39) Kim, A.; Lee, H.; Park, J.; Kang, H.; Yang, H.; Song, H.; Park, K. Highly efficient and reusable copper-catalyzed N-arylation of nitrogen-containing heterocycles with aryl halides. *Molecules* **2009**, *14*, 5169−5178.
(40) Rout, L.; Jammi, S.; Punniyamurthy, T. Novel CuO nanoparticle catalyzed C−N cross coupling of amines with iodobenzene. *Org. Lett.* **2007**, *9*, 3397−3399.
(41) Huang, Y.; Miao, H.; Zhang, Q.; Chen, C.; Xu, J. Cu_2O: A simple and efficient reusable catalyst for N-arylation of nitrogen-containing heterocycles with aryl halides. *Catal. Lett.* **2008**, *122*, 344−348.